eNeuro

Research Article: New Research
Integrative Systems

Alpha-Frequency Stimulation Enhances Synchronization of Alpha Oscillations with Default Mode Network Connectivity

Yijia Ma,[1,2]* Joshua A. Brown,[1,2]* Chaowen Chen,[1] Mingzhou Ding,[3] Wei Wu,[4] and Wen Li[1,2]

[1]Louis A. Faillace, MD, Department of Psychiatry and Behavioral Sciences, University of Texas Health Science Center, Houston, Texas 77030, [2]Department of Psychology, Florida State University, Tallahassee, Florida 32306, [3]J Crayton Pruitt Family Department of Biomedical Engineering, University of Florida, Gainesville, Florida 32611, and [4]Department of Statistics, Florida State University, Tallahassee, Florida 32306

Abstract

Alpha (8–12 Hz) oscillations and default mode network (DMN) activity dominate the brain's intrinsic activity in the temporal and spatial domains, respectively. They are thought to play crucial roles in the spatiotemporal organization of the complex brain system. Relatedly, both have been implicated, often concurrently, in diverse neuropsychiatric disorders, with accruing electroencephalogram (EEG)/magnetoencephalogram and functional magnetic resonance imaging (fMRI) data linking these two neural activities both at rest and during key cognitive operations. Prominent theories and extant findings thus converge to suggest a mechanistic relationship between alpha oscillations and the DMN. Here, we leveraged simultaneous EEG–fMRI data acquired before and after alpha-frequency transcranial alternating current stimulation (α-tACS) and observed that α-tACS tightened the dynamic coupling between spontaneous fluctuations in alpha power and DMN connectivity (especially, in the posterior DMN, between the posterior cingulate cortex and the bilateral angular gyrus). In comparison, no significant changes were observed for temporal correlations between power in other oscillatory frequencies and connectivity in other major networks. These results thus suggest an inherent coupling between alpha and DMN activity in humans. Importantly, these findings highlight the efficacy of α-tACS in regulating the DMN, a clinically significant network that is challenging to target directly with noninvasive methods.

Key words: alpha oscillations; brain stimulation; default mode network; dynamic coupling

Significance Statement

Alpha (8–12 Hz) oscillations and the default mode network (DMN) represent two major intrinsic activities of the brain. Prominent theories and extant findings converge to suggest a mechanistic relationship between alpha oscillations and the DMN. Combining simultaneous electroencephalogram–functional magnetic resonance imaging with alpha-frequency transcranial alternating current stimulation (α-tACS), we demonstrated tightened coupling between alpha oscillations and DMN connectivity. These results lend credence to an inherent alpha–DMN link. Given DMN dysfunctions in multiple major neuropsychiatric conditions, the findings also highlight potential utility of α-tACS in clinical interventions by regulating the DMN.

Introduction

Research using resting-state (RS) electroencephalography (EEG), magnetoencephalography (MEG), and functional magnetic resonance imaging (fMRI) recordings has reliably depicted the temporal and spatial landscapes of intrinsic activities in the human brain.

Received Oct. 21, 2024; revised Jan. 29, 2025; accepted Jan. 31, 2025.

The authors declare no competing financial interests.

Author contributions: Y.M., J.A.B., C.C., M.D., W.W., and W.L. designed research; Y.M., J.A.B., W.W., and W.L. performed research; Y.M. and J.A.B. analyzed data; Y.M., J.A.B., and W.L. wrote the paper.

This research was supported by the National Institutes of Health Grants (R01MH132209 and R01NS129059 to W.L.).

*Y.M. and J.A.B. contributed equally to this work.

Correspondence should be addressed to Yijia Ma at Yijia.Ma@uth.tmc.edu or Wen Li at wen.li.1@uth.tmc.edu.

Temporally, as revealed by EEG/MEG, the resting brain is dominated by oscillatory activities in the range of 8–12 Hz (known as alpha oscillations), representing the main rhythm of intrinsic neural synchronization (Klimesch et al., 2007; Palva and Palva, 2007). Spatially, as demonstrated by fMRI, the resting brain is characterized by widely distributed coactivation anchored in a midline core comprising the posterior cingulate cortex (PCC) and the medial prefrontal cortex (mPFC), along with the left and right angular gyri (l/r AG), collectively forming the default mode network (DMN; Raichle and Snyder, 2007; Buckner and DiNicola, 2019).

Both the DMN and alpha oscillations underpin the dynamic organization of the brain. Through long-range synchrony and coactivation, alpha oscillations and the DMN can temporally and spatially orchestrate neural processes on meso- and macroscopic levels, constituting pivotal architectures of the brain's intrinsic organization (Varela et al., 2001; Buzsáki and Draguhn, 2004; Shanahan, 2010; Deco and Corbetta, 2011). As such, alpha oscillations and the DMN are both strongly implicated in fundamental cognitive operations, including consciousness, awareness, and vigilance (Sadaghiani and Kleinschmidt, 2016; Buckner and DiNicola, 2019). Similarly, their dysfunctions have been linked to the pathophysiology of major neuropsychiatric disorders, including Alzheimer's disease, schizophrenia, and post-traumatic stress disorder (PTSD), representing fundamental, transdiagnostic pathological underpinnings (Greicius et al., 2004; Osipova et al., 2005; Whitfield-Gabrieli et al., 2009; Akiki et al., 2017; Clancy et al., 2017; Tu et al., 2019; Clancy et al., 2020a).

Akin to these prominent parallels between them, growing evidence suggests that alpha oscillations and the DMN are inherently and mechanistically associated (Tagliazucchi et al., 2012; Tang et al., 2017). Research combining high-density EEG/MEG with fMRI or source localization indicates that alpha oscillations represent the primary neural synchrony linking the core hubs (mPFC and PCC) of the DMN (Hillebrand et al., 2016; Tang et al., 2017; Coito et al., 2019; Samogin et al., 2019). In PTSD, this alpha-oscillatory connectivity between the DMN midline hubs is deficient, underscoring the joint alpha–DMN pathology (Clancy et al., 2020b). In addition, alpha oscillations and DMN activity are highly dynamic, fluctuating ("waxing and waning") spontaneously over time (Lopes da Silva and Niedermeyer, 2005; Kucyi et al., 2016). Research has leveraged these temporal dynamics to directly link alpha and DMN activities: simultaneous EEG–fMRI recordings have repeatedly revealed that the spontaneous fluctuations in alpha oscillations and DMN activity are temporally coupled (Jann et al., 2009; Knyazev et al., 2011; Scheeringa et al., 2012; Mo et al., 2013; Samogin et al., 2019), thereby highlighting a direct linkage.

Recently, using transcranial alternating current stimulation (tACS) at the alpha frequency to augment alpha oscillations, research has further demonstrated that alpha enhancement leads to the upregulation of DMN connectivity and activation (Clancy et al., 2022; Kasten and Herrmann, 2022). These findings thus highlight a mechanistic alpha–DMN association, with shared neural underpinnings that are responsive to alpha-frequency tACS (α-tACS). By that token, we hypothesized that by upregulating the shared neural underpinnings, α-tACS would not only result in the concurrent enhancement of alpha and DMN activity but also tighten their temporal coupling. Evidence for this hypothesis would lend further credence to the potentially mechanistic linkage between alpha oscillations and the DMN. Importantly, it would constitute a mechanistic foundation for noninvasive brain stimulation such as α-tACS to upregulate these two systems, which both figure critically in mental functioning and its various disorders.

Therefore, this study sought to directly examine the effect of α-tACS on the temporal coupling of spontaneous alpha and DMN fluctuations. Toward that end, we reanalyzed data from Clancy et al. (2022), where RS EEG and fMRI were simultaneously recorded before and after 20 min of occipitoparietal α-tACS. Extracting the time series of alpha power and DMN connectivity and comparing their correlation (reflecting the temporal coupling) before and after stimulation, we tested the hypothesis that the coupling of alpha and DMN fluctuations would increase after α-tACS.

Materials and Methods

Participants

Data from a prior study (Clancy et al., 2022) were reanalyzed to test the hypotheses. Thirty-two healthy participants (17 females; age 20.9 ± 3.5 years), who had simultaneous EEG–fMRI data, were included in the current study. Participants had no prior history of neurological or psychiatric disorders or use of psychotropic medications at the time of recruitment. Participants were randomly assigned to receive either active tACS stimulation ($n = 16$) or sham stimulation ($n = 16$). Groups did not differ in age or gender distribution (p's > 0.3).

Experimental procedures

The experiment consisted of three phases: prestimulation RS recordings, tACS/sham stimulation, and poststimulation RS recordings (Fig. 1*A*). In both pre- and poststimulation phases, participants underwent two successive 5 min (10 min in total) simultaneous EEG–fMRI scans (with eyes open and fixated on a central crosshair). α-tACS was administered for 20 min, with a ±2 mA sinusoidal current oscillating at 10 Hz using an MR-compatible high-definition (HD) tACS system (Soterix Medical). A 4 × 1 montage over midline occipitoparietal sites (with 4 surrounding +1 central electrodes forming a closed circuit) was selected to maximally target the primary cortical source of alpha oscillations—occipitoparietal cortex (Klimesch et al., 2007; Palva and Palva, 2007; Clancy et al., 2018). More details are reported in Clancy et al. (2022).

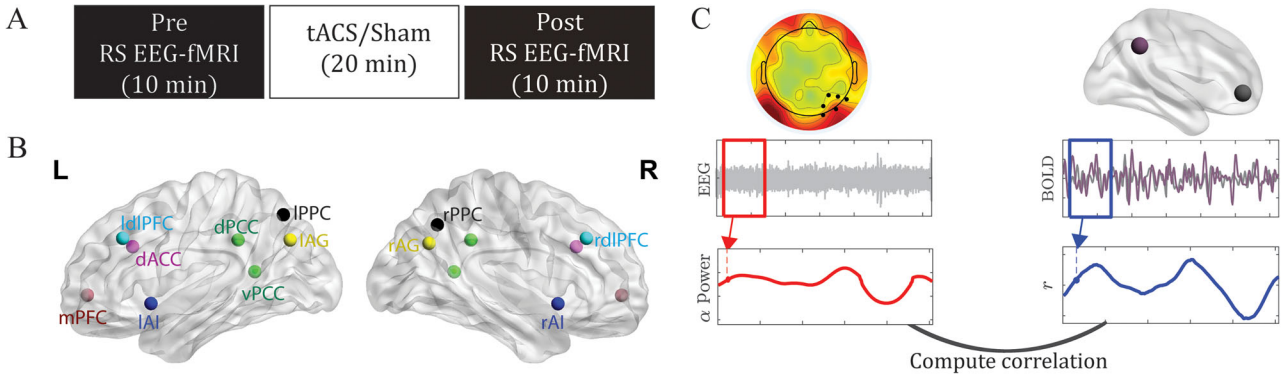

Figure 1. Experimental paradigm (***A***), ROIs (***B***), and dynamic analysis pipeline (C). ***A***, Experimental design. Participants underwent simultaneous RS EEG–fMRI recordings before and after tACS/sham stimulation. Each recording session lasts 10 min. ***B***, ROIs. Abbreviations: (l/r) AI, (left/right) anterior insula; dACC, dorsal anterior cingulate cortex; (l/r) dlPFC, (left/right) dorsolateral prefrontal cortex; (d/v) PCC, (dorsal/ventral) posterior cingulate cortex; (l/r) PPC, (left/right) posterior parietal cortex; mPFC, medial prefrontal cortex; (l/r) AG, (left/right) angular gyrus. ***C***, Analysis pipeline illustrating the methods used (see text for more details).

fMRI acquisition and preprocessing

fMRI data were acquired in a 3 T Siemens Prisma scanner with a 64-channel head coil and axial acquisition. Imaging parameters included TR/TE, 1,800/22.40 ms; slice thickness, 1.8 mm; gap, 0.45 mm; in-plane resolution/voxel size, 1.8 × 1.8 mm; multiband acceleration factor, 2; and generalized autocalibrating partial parallel acquisition acceleration factor, 2. A high-resolution ($0.9 \times 0.9 \times 0.9$ mm^3) three-dimensional magnetization-prepared rapid acquisition gradient echo (3D-MPRAGE) T1 scan was also acquired. Following discarding dummy scans (the first nine volumes of each block), data of the two blocks were concatenated.

Imaging data were preprocessed using SPM12, including slice-time correction, spatial realignment, and normalization using diffeomorphic anatomical registration through exponentiated lie (DARTEL) algebra. To further remove artifacts potentially contributing to spurious RS activity variance (Power et al., 2012), we implemented additional preprocessing using the Data Processing Assistant for Resting-State fMRI toolbox: (1) mean centering and whitening of timeseries; (2) temporal bandpass (0.01–0.08 Hz) filtering; and (3) general linear modeling to partial out head motion with 24 nuisance variables (six head motion parameters each from the current and previous scan and their squared values).

Regions of interest (ROIs). ROIs were selected from the hubs of three major intrinsic connectivity networks, namely, the DMN, executive control network (ECN), and salience network (SN). The ECN and SN were included as control networks to elucidate whether alpha oscillations are specifically coupled with the DMN.

We defined these ROIs primarily based on the 90 functional ROI Willard Atlas (Altmann et al., 2015). DMN ROIs included the ventro-mPFC, the PCC, and the l/r AG. As in the previous study (Clancy et al., 2022), given that the PCC hub consists of two functionally dissociable, ventral and dorsal, subdivisions (with the ventral PCC/vPCC primarily linked with DMN nodes and the dorsal PCC/dPCC with extensive extra-DMN connections (Leech et al., 2011; Buckner and DiNicola, 2019)), we defined the vPCC and dPCC individually from the Brainnetome Atlas (Fan et al., 2016). ECN ROIs included the left and right dorsolateral prefrontal cortex and posterior parietal cortex (l/r PPC). SN ROIs included the dorsal anterior cingulate cortex and the left and right anterior insula (Fig. 1*B*).

EEG acquisition and preprocessing

EEG data were recorded using an MR-compatible 64–channel system (Brain Products). An additional electrode was placed on the participant's back to record electrocardiogram, allowing for the removal of cardiac artifacts from the EEG data. Detailed information about data acquisition, preprocessing, and artifact removal is provided in Clancy et al. (2022). The cleaned EEG data were segmented into epochs of 1.8 s (i.e., the TR length) centered on the onset of each fMRI scan (TR).

Oscillatory power was computed at individual channels for each epoch using the multitaper spectral estimation technique with three tapers (Park et al., 1987; Mitra and Pesaran, 1999). Alpha (8–12 Hz) power was extracted from the right occipitoparietal site (collapsed across P4, P6, P8, PO4, PO8, and O2) which demonstrated the strongest alpha increase following *α*-tACS (Clancy et al., 2022; Fig. 1*C*). These values were then normalized by the mean power for the global spectrum (1–40 Hz). To determine alpha-frequency–specific effects, power was similarly derived for the neighboring frequencies, theta (4–7 Hz), and low beta (13–17) bands and submitted to similar analyses.

Dynamic analysis

To examine the temporal coupling between alpha oscillations and DMN connectivity, we measured the covariation of fluctuations of these two activities over time. We implemented a tapered sliding window approach as commonly used

in previous studies (Richiardi et al., 2011; Shirer et al., 2012; Allen et al., 2014). We used a Gaussian window, with smoothing kernel/FWHM of 27.78 epochs and a length of 108 s (60 epochs), resulting in a frequency threshold of 0.01 Hz. This threshold, corresponding to the lower bound of the RS BOLD activity, has been commonly used (Fransson, 2005; Chen and Glover, 2015; Leonardi and Van De Ville, 2015; Preti et al., 2017; Pedersen et al., 2018; Vergara et al., 2019). To ensure sufficient temporal resolution, we selected sliding increments of 1.8 s (1 TR), which resulted in 247 windows (i.e., time points) with an overlap of 106.2 s (59 TR) between neighboring windows (Tagliazucchi et al., 2012; Shakil et al., 2016; Li et al., 2022).

We extracted BOLD signals from every ROI within each Gaussian window and computed the functional connectivity between the ROIs for each window. We convolved EEG power per epoch with the Gaussian window to generate the EEG power timeseries. We measured the covariation between fluctuations of fMRI connectivity and oscillatory power by extracting Pearson's correlation coefficients between the fMRI functional connectivity timeseries and EEG power timeseries. Following previous work (Chang et al., 2013), we avoided convolving the EEG power timeseries with a hemodynamic response function such that its amplitude values would be preserved without potential distortions. To assess whether the inherent time resolutions between imaging modalities affected the results, we performed validation analyses varying the offset between EEG and fMRI. Figure 1 illustrates the procedures of this analysis. All computations were performed using in-house MATLAB scripts, relying solely on built-in functions, except for notBoxPlot (https://github.com/raacampbell/notBoxPlot/) for visualization and select EEGLAB functions (Delorme and Makeig, 2004) for EEG data processing.

Statistical analysis

To test our hypothesis that tACS would enhance the dynamic coupling between alpha oscillations and DMN connectivity, we submitted Pearson's correlation coefficients (after Fisher Z transformation) to double contrasts: Post–$\text{Pre}_{(\text{Active-Sham})}$. Specifically, for each double contrast, we subtracted each participant's poststimulation Z transformed r value from their prestimulation r value and entered the differential r value into two-sample t tests between the active and sham groups. Basic assumptions of these t tests, including normality and homogeneity, were verified statistically. The double contrasts were corrected for multiple comparisons across the DMN hubs, based on FDR $p < 0.05$. We followed up the significant double contrasts with simple t tests to unpack the effects. As these simple contrasts were restricted to (and hence, protected by) the significant double contrasts, we did not apply further corrections (to prevent overcorrection that could increase Type 2 errors). For the same reason, we also used one-tailed $p < 0.05$ for the simple contrasts.

Results

α-tACS enhanced alpha–DMN coupling

Our double contrasts indicated an increase in the coupling between alpha power and vPCC–lAG connectivity timeseries in the active (vs sham) group after stimulation ($t = 3.14$; FDR $p = 0.038$; Fig. 2). Specifically, the active group showed an increase ($t = 2.57$; $p = 0.011$; one-tailed), while the sham group showed a decrease ($t = -1.79$; $p = 0.046$; one-tailed) in this coupling. Our double contrasts also showed an increase in the coupling between alpha power and vPCC–rAG connectivity timeseries in the active (vs sham) group ($t = 2.76$; FDR $p = 0.048$) after stimulation. Specifically, the active group exhibited an increase ($t = 1.82$; $p = 0.045$; one-tailed) compared with the sham group with a decrease ($t = -2.16$; $p = 0.023$; one-tailed) in this coupling. Nuances of such effects are illustrated in Figure 3, based on data from a representative participant in the active group. Finally, our control analyses below further ruled out a possible confound of global temporal association between EEG–fMRI connectivity (Fig. 5).

Effects were specific to the alpha frequency and DMN

To ascertain whether the coupling was specific to the alpha frequency, we performed similar tests on theta and beta frequencies. We observed no effect of α-tACS on these couplings (FDR p's > 0.2; Fig. 4*A*).

To evaluate whether the coupling was specific to the DMN, we performed similar double contrasts on connectivity of the other major networks—the CEN and SN. As illustrated in Figure 4*B*, there were no effects of tACS on these couplings (FDR p's > 0.09).

Effects were consistent across different lags

Finally, we examined the potential effect of the lag size on the alpha–DMN dynamic coupling to consider the sluggishness of fMRI relative to EEG indices for neural activity (Boynton et al., 1996; Liu and He, 2008). We varied the lag from zero to five TRs (1.8–9 s), and as illustrated in Figure 4*C*, the results for vPCC–rAG and vPCC–lAG remained significant across the range (FDR p's < 0.05).

Control analysis

Controlling for alpha association with global connectivity fluctuations

To highlight the dynamic coupling of alpha with intra-DMN connectivity and control for global changes in DMN connectivity, we extracted the timeseries of extra-DMN connectivity between any of the DMN nodes with any of the CEN and SN

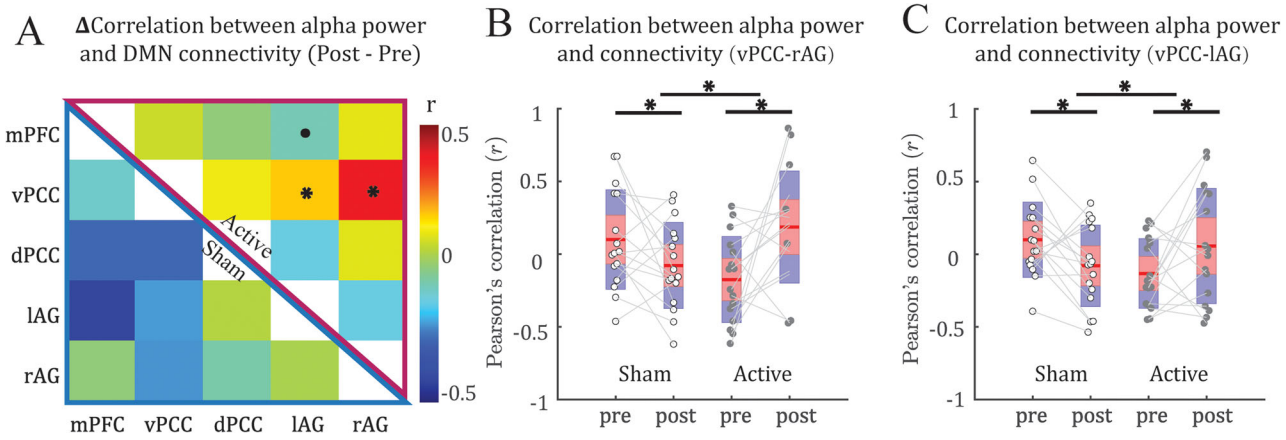

Figure 2. α-tACS strengthened dynamic coupling between DMN connectivity and alpha power. ***A***, Mean changes (Post–Pre) in the dynamic coupling matrix for the active (top right) and sham control (bottom left) groups across subjects. ***B***, ***C***, Boxplots illustrate increased coupling (from Pre to Post) between fluctuation of alpha power and PCC–rAG (***B***) and PCC–lAG (***C***) connectivity in the active (vs sham) group. The red- and blue-shaded areas correspond to the mean ± 1.96 × SEM and the mean ± 1.96 × SD, respectively. For the double contrasts, * = $p < 0.05$ FDR corrected; $p < 0.1$ FDR corrected. For the follow-up simple contrasts, $p < 0.1$; *$p < 0.05$. The dynamic coupling between alpha power and connectivity of DMN with the CEN and SN, and baseline alpha–DMN coupling are shown in Extended Data Figures 2-1 and 2-2, respectively.

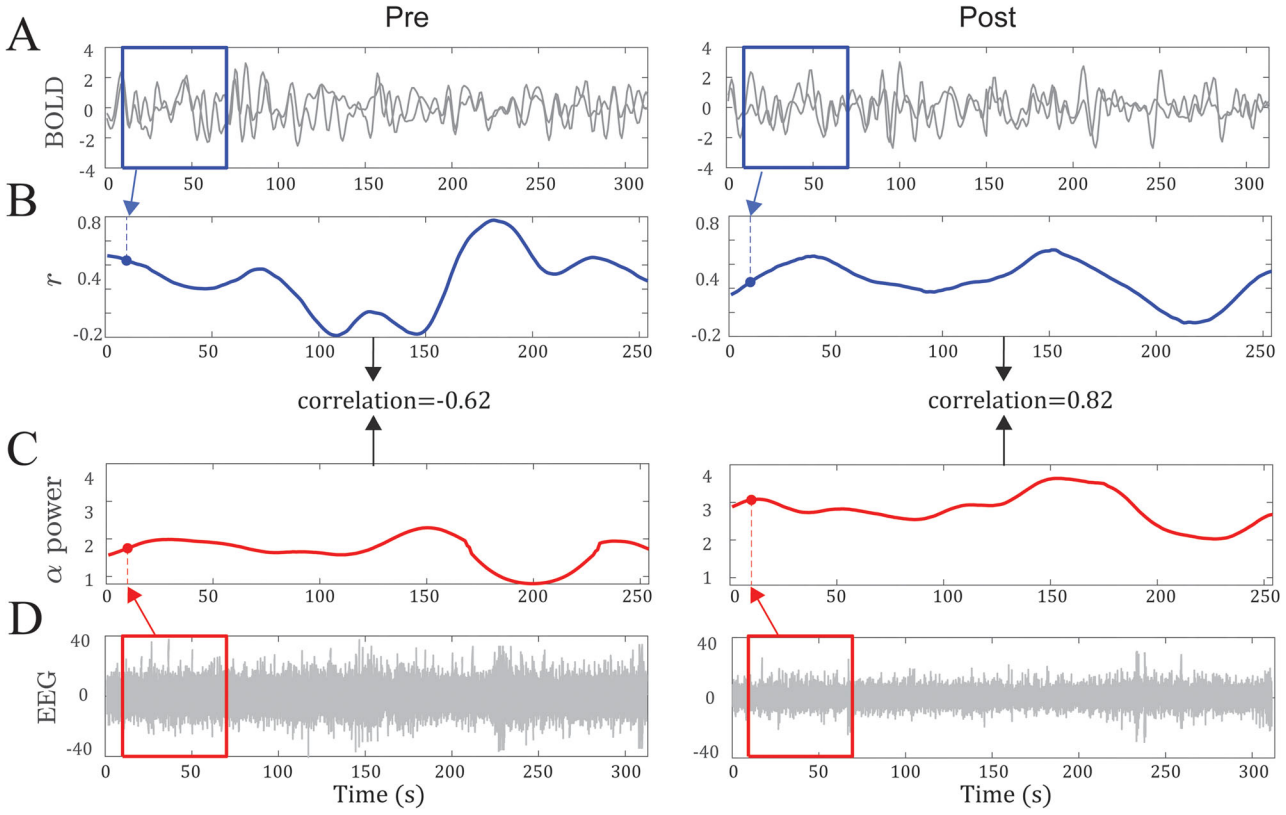

Figure 3. Data from a representative participant. ***A***, ***B***, For each pair of ROIs (here, vPPC and right AG), average BOLD signals were extracted using a sliding Gaussian window of 60 TRs (~2 min; ***A***). The two BOLD timeseries for each sliding window were then correlated, resulting in a *r* coefficient (i.e., FC strength). Congregating the *r* values for all windows (sliding in increments of 1 TR) across the Pre (left) and Post (right) recordings, we obtained the respective FC timeseries (***B***). ***C***, ***D***, Similarly, we obtained an alpha power timeseries for the Pre (left) and Post (right) sessions (***C***). Specifically, we extracted alpha power from each sliding window and congregated alpha power from all windows for Pre and Post sessions, respectively (***D***). Finally, we correlated the timeseries of FC and alpha power for each session (***B***, ***C***) and obtained an index of dynamic alpha–FC coupling. In this participant, the coupling increased from −0.62 Pre (left) to 0.82 Post (right).

nodes. We then subtracted the averaged correlation coefficients between alpha and extra-DMN connectivity timeseries from the corresponding correlation coefficients between alpha and intra-DMN connectivity and submitted the differential (i.e., adjusted) coefficients to the double contrasts for hypothesis testing.

We confirmed increase in dynamic coupling between alpha power and the adjusted vPCC–rAG FC in the active (vs sham) group ($t = 3.8$; FDR $p = 0.006$) after stimulation (Fig. 5). Specifically, the active group showed an increase ($t = 3.35$; $p = 0.002$; one-tailed), while the sham group showed a decrease ($t = -1.91$; $p = 0.038$ one-tailed) in this coupling. We also found an increase in coupling between fluctuations of alpha power and the adjusted vPCC–lAG connectivity in the active (vs Sham) group ($t = 2.75$; FDR $p = 0.033$) after stimulation. Specifically, the active group showed an increase ($t = 1.75$; $p = 0.049$; one-tailed), while the sham group showed a decrease ($t = -2.19$; $p = 0.022$; one-tailed) in this coupling. Moreover, we found an increase in coupling between fluctuations of alpha power and mPFC–lAG connectivity in the active (vs sham) group ($t = 2.81$; FDR $p = 0.033$) after stimulation. Specifically, the active group showed no difference ($t = -0.27$; $p = 0.39$; one-tailed), while the sham group showed a decrease ($t = -3.96$; $p < 0.001$; one-tailed) in this coupling.

Between-network connectivity effects

For completeness, we also examined the effects of tACS on EEG–fMRI coupling for between-network connectivity. tACS effects on the adjusted DMN connectivity were not observed for connectivity between DMN and CEN/SN (p's > 0.05 FDR corrected). Notably, there was no effect of tACS for connectivity between the posterior DMN (PCC, r/l AG) and the posterior CEN (r/l PPC). A detailed picture illustration is available in Extended Data Figure 2-1.

Baseline alpha–DMN coupling

Pooling prestimulation baseline data from the active and sham groups, we examined the baseline coupling between alpha and DMN connectivity timeseries. However, there was no reliable coupling between them (p's > 0.1). A detailed picture illustration is available in Extended Data Fig. 2-2.

Discussion

Alpha oscillations and the DMN represent the dominant activities of RS EEG/MEG and fMRI, respectively. They are thought to play crucial roles in the spatiotemporal organization of the complex brain system, both figuring importantly in fundamental cognitive processes and implicated, often concurrently, in diverse neuropsychiatric disorders. Leveraging simultaneous EEG–fMRI data acquired before and after α-tACS, we demonstrated tightening of the coupling between temporal fluctuations in alpha power and DMN connectivity (particularly, in the posterior DMN between PCC and bilateral AG). Importantly, we systematically ruled out the effect of α-tACS on the coupling between fluctuations in beta and theta oscillations and in other major large-scale networks (the CEN and SN). In addition, findings were consistent across different time lags between fMRI and EEG timeseries, indicating the robustness of this alpha–DMN coupling. Therefore, the perturbation of alpha oscillations via α-tACS caused specific and robust impacts on the alpha–DMN coupling, highlighting an inherent association between these two major intrinsic neural activities. Moreover, the efficacy of α-tACS in enhancing this association provides support for tACS-based therapeutics in clinical interventions.

Functional connectivity and neural oscillations both fluctuate over time, and such dynamics bear significant behavioral and clinical relevance (Lopes da Silva and Niedermeyer, 2005; Hutchison et al., 2013; Lurie et al., 2020). Accordingly, establishing a specific coupling between fluctuations in alpha and DMN connectivity would support an inherent association between alpha oscillations and the DMN. However, to date, only a handful of studies have leveraged simultaneous EEG–fMRI to perform direct investigation of such a coupling (Tagliazucchi et al., 2012; Chang et al., 2013). Moreover, while this literature has demonstrated a negative coupling between fluctuations in RS alpha oscillations and between-network (e.g., DMN–CEN) connectivity, it has failed to uncover a reliable coupling between alpha power and DMN connectivity. We suspect that this coupling may be obscured by the various artifacts inherent in RS recordings, necessitating more powerful methods for its detection. α-tACS is an effective tool to modulate alpha oscillations (Antal and Paulus, 2013; Herrmann et al., 2013), experimentally perturbing its fluctuations and putatively, its coupling with the DMN. Indeed, by combining it with simultaneous EEG–fMRI, we garnered evidence for the alpha–DMN connectivity coupling.

Interestingly, this coupling appears largely confined to the posterior DMN (between the PCC and the AG). Given that α-tACS was administered at the posterior scalp, targeting the occipitoparietal cortex, it is possible that this effect in the posterior DMN merely arose from a posterior alpha entrainment by α-tACS. However, α-tACS did not produce such an effect for connectivity between the posterior DMN nodes (PCC, left/right ANG) and the posterior node of the CEN (l/r PPC), thereby ruling out this explanation. While both are integral hubs of the DMN, the mPFC and PCC exhibit opposite connectivity patterns with other networks and show opposite responses during tasks, suggesting that they are dissociable subdivisions of the DMN (Raichle et al., 2001; Buckner and DiNicola, 2019). Functionally, the PCC (and the posterior DMN) is believed to perform broad-based continuous sampling of external and internal environments (Raichle et al., 2001). Relatedly, alpha oscillations play a significant role in modulating sensory processing and maintaining vigilance (Klimesch et al., 2007; Palva and Palva, 2007). Therefore, there may be a special intimacy between alpha oscillations and the posterior DMN, which are inherently coupled to synergistically facilitate and regulate sensory sampling and vigilance. Sensory processing and vigilance were not examined in the current study to confirm this implication. However,

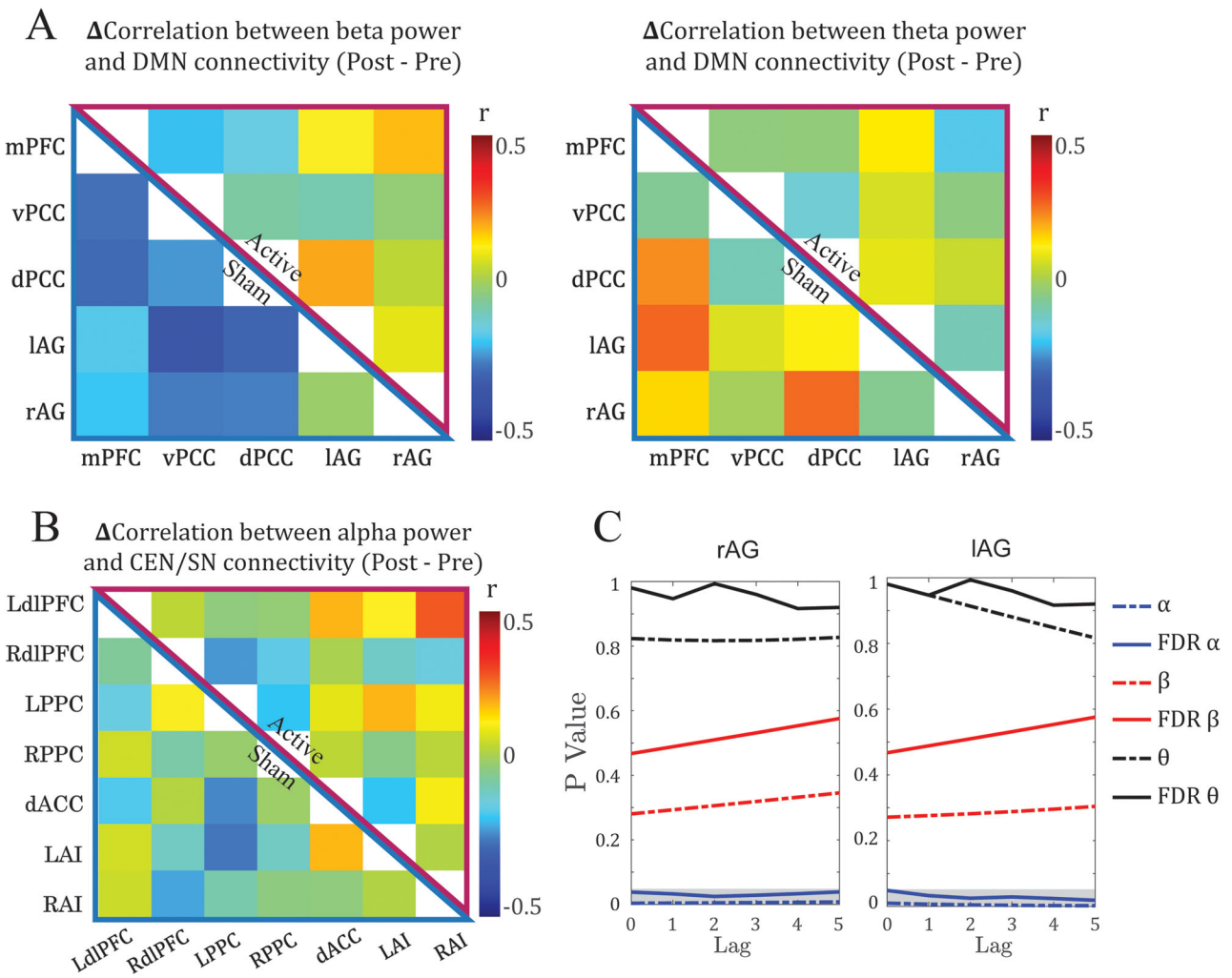

Figure 4. α-tACS modulation of dynamic coupling across brain networks and frequency bands. ***A,*** No effect of α-tACS on the dynamic coupling between DMN connectivity and beta or theta power. Mean differential (Post–Pre) dynamic coupling matrices were comparable between active (top right) and sham (bottom left) groups for beta (**left**) and theta (**right**) band power. ***B***, No effect of α-tACS on the dynamic coupling between alpha power and CEN/SN connectivity. Mean differential (Post–Pre) dynamic coupling matrix of connectivity within and between CEN and SN was comparable between active (top right) and sham (bottom left) groups. No effects survived the significance threshold ($p < 0.05$ FDR corrected). ***C***, Effects of the lag size. *P* and corrected *p* values for the effect of tACS on the dynamic coupling of alpha (blue lines) with vPCC–rAG (left) and vPCC–lAG (right) connectivity were consistently significant (gray shaded area) over lags of zero to five TRs. In contrast, beta (red lines) and theta (black lines) showed stable, nonsignificant patterns over the same lags.

previous research (Clancy et al., 2018) has demonstrated the effect of *α*-tACS in modulating sensory processing and reducing anxious arousal, lending support to this notion.

Further in line with this idea, alpha oscillations and the DMN may share a fundamental anatomical substrate—the thalamocortical circuitry (Halassa and Sherman, 2019). This circuitry has long been known to generate and regulate alpha oscillations (Buzsaki et al., 2013; Crunelli et al., 2015). Recently, it has also been considered as a key controller of the DMN (Buckner and DiNicola, 2019). The thalamocortical circuitry, encompassing the thalamus, sensory cortex, and thalamic reticular nucleus, is a primary machinery for basic sensory processing. In addition, it is crucial for the control and regulation of arousal and vigilance (McCormick and Bal, 1997). Therefore, the coupling between alpha and DMN activity can arise from the thalamocortical circuitry to facilitate cooperation in sensory sampling and vigilance. Moreover, the effect of psilocybin, a serotonin agonist (Vollenweider and Preller, 2020), can increase both alpha power and posterior DMN connectivity, implicating a neurochemical (serotoninergic) basis for the alpha–DMN coupling. Particularly, the serotonergic system plays a pivotal role in sensory processing and vigilance (Davis et al., 1986; Hurley et al., 2004), reinforcing the idea that alpha and DMN are inherently coupled to maintain vigilance in concert with environmental stimuli. Consequently, as the levels of sensory sampling and vigilance spontaneously wax and wane over time, alpha and DMN activity in RS recordings rises and falls in synchrony, manifesting as a tight temporal coupling.

The study has several limitations that need to be addressed in future research. First, as illustrated in Figure 2, the active and sham groups differed in baseline levels of alpha–DMN coupling. This could be a random sampling error as a result of

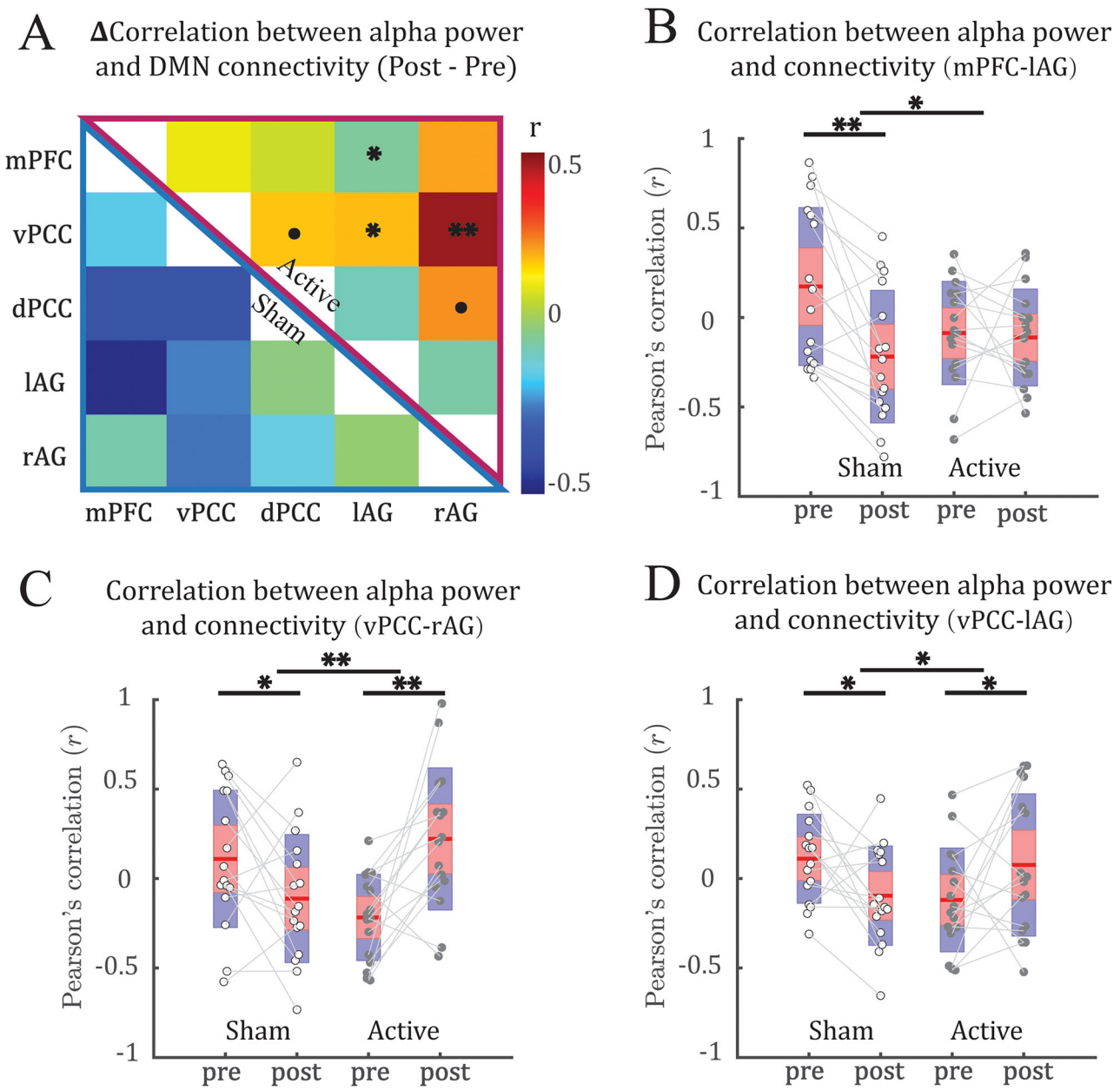

Figure 5. α-tACS strengthened dynamic coupling between adjusted DMN connectivity and alpha power. ***A***, Changes (Post–Pre) in the dynamic coupling matrix for the active (top right) and sham control (bottom left) groups. ***B–D***, Boxplots illustrate increased coupling (from Pre to Post) between fluctuation of alpha power with mPFC–lAG connectivity (***B***), PCC–rAG connectivity (***C***) and PCC–lAG connectivity (***D***) in the active (vs Sham) group. The red- and blue-shaded areas correspond to the mean ± 1.96 × SEM and the mean ± 1.96 × SD, respectively. For the double contrasts, $p < 0.1$ FDR corrected; *$p < 0.05$ FDR corrected. **$p < 0.01$ FDR corrected. For the follow-up simple contrasts, ·$p < 0.1$ uncorrected; *$p < 0.05$ uncorrected; **$p < 0.01$ uncorrected.

our modest sample size ($N = 32$). That said, this difference may not present a major confound and obscure our hypothesis as the two groups showed opposite changes after stimulation, with the sham group showing a decline in coupling overtime, while the active group exhibited an increase. Namely, tACS could overcome a general decline overtime and increase the alpha–DMN coupling. Second, potential confounding factors driving both DMN connectivity and alpha power include respiration and arousal, which naturally occur during rest and are often treated as noise in fMRI studies (Glover et al., 2000; Birn et al., 2006; Behzadi et al., 2007; Chang et al., 2009). However, these fluctuations may have neural correlates, as suggested by significant correlations observed between alpha EEG power, respiration, and BOLD signals (Yuan et al., 2013; Korponay et al., 2024). Future research should incorporate specific measurements of such physiological variations to more specifically elucidate the relationship between alpha power and DMN connectivity.

In conclusion, by combining simultaneous EEG–fMRI timeseries and neural perturbation via α-tACS, we identified a specific temporal coupling between alpha oscillations and DMN connectivity. This finding lends further credence to an

inherent, potentially mechanistic relationship between alpha oscillations and the DMN. Notably, the isolation of the posterior DMN in this coupling raises an intriguing possibility that this alpha–DMN coupling could bear particular relevance to sensory vigilance. Clinically, the efficacy of α-tACS in tightening alpha–DMN coupling presents new opportunities to noninvasively enhance neural functioning and treat mental disorders, especially those involving hypervigilance and sensory anomalies, such as post-traumatic stress disorder.

References

Akiki TJ, Averill CL, Abdallah CG (2017) A network-based neurobiological model of PTSD: evidence from structural and functional neuroimaging studies. Curr Psychiatry Rep 19:81.

Allen EA, Damaraju E, Plis SM, Erhardt EB, Eichele T, Calhoun VD (2014) Tracking whole-brain connectivity dynamics in the resting state. Cereb Cortex 24:663–676.

Altmann A, Ng B, Landau SM, Jagust WJ, Greicius MD (2015) Regional brain hypometabolism is unrelated to regional amyloid plaque burden. Brain 138:3734–3746.

Antal A, Paulus W (2013) Transcranial alternating current stimulation (tACS). Front Hum Neurosci 7:318.

Behzadi Y, Restom K, Liau J, Liu TT (2007) A component based noise correction method (CompCor) for BOLD and perfusion based fMRI. Neuroimage 37:90–101.

Birn RM, Diamond JB, Smith MA, Bandettini PA (2006) Separating respiratory-variation-related fluctuations from neuronal-activity-related fluctuations in fMRI. Neuroimage 31:1536–1548.

Boynton GM, Engel SA, Glover GH, Heeger DJ (1996) Linear systems analysis of functional magnetic resonance imaging in human V1. J Neurosci 16:4207–4221.

Buckner RL, DiNicola LM (2019) The brain's default network: updated anatomy, physiology and evolving insights. Nat Rev Neurosci 20:593–608.

Buzsáki G, Draguhn A (2004) Neuronal oscillations in cortical networks. Science 304:1926–1929.

Buzsaki G, Logothetis N, Singer W (2013) Scaling brain size, keeping timing: evolutionary preservation of brain rhythms. Neuron 80:751–764.

Chang C, Cunningham JP, Glover GH (2009) Influence of heart rate on the BOLD signal: the cardiac response function. Neuroimage 44:857–869.

Chang C, Liu Z, Chen MC, Liu X, Duyn JH (2013) EEG correlates of time-varying BOLD functional connectivity. Neuroimage 72:227–236.

Chen JE, Glover GH (2015) BOLD fractional contribution to resting-state functional connectivity above 0.1 Hz. Neuroimage 107:207–218.

Clancy KJ, Albizu A, Schmidt NB, Li W (2020a) Intrinsic sensory disinhibition contributes to intrusive re-experiencing in combat veterans. Sci Rep 10:936.

Clancy KJ, Andrzejewski JA, Simon J, Ding M, Schmidt NB, Li W (2020b) Posttraumatic stress disorder is associated with a dysrhythmia across the visual cortex and the default mode network. eNeuro 7:1.

Clancy KJ, Andrzejewski JA, You Y, Rosenberg JT, Ding M, Li W (2022) Transcranial stimulation of alpha oscillations upregulates the default mode network. Proc Natl Acad Sci U S A 119:e2110868119.

Clancy KJ, Baisley SK, Albizu A, Kartvelishvili N, Ding M, Li W (2018) Lasting connectivity increase and anxiety reduction via transcranial alternating current stimulation. Soc Cogn Affect Neurosci 13:1305–1316.

Clancy K, Ding M, Bernat E, Schmidt NB, Li W (2017) Restless 'rest': intrinsic sensory hyperactivity and disinhibition in post-traumatic stress disorder. Brain 140:2041–2050.

Coito A, Michel CM, Vulliemoz S, Plomp G (2019) Directed functional connections underlying spontaneous brain activity. Hum Brain Mapp 40:879–888.

Crunelli V, David F, Lorincz ML, Hughes SW (2015) The thalamocortical network as a single slow wave-generating unit. Curr Opin Neurobiol 31:72–80.

Davis M, Cassella JV, Wrean WH, Kehne JH (1986) Serotonin receptor subtype agonists: differential effects on sensorimotor reactivity measured with acoustic startle. Psychopharmacol Bull 22:837–843.

Deco G, Corbetta M (2011) The dynamical balance of the brain at rest. Neuroscientist 17:107–123.

Delorme A, Makeig S (2004) EEGLAB: an open source toolbox for analysis of single-trial EEG dynamics including independent component analysis. J Neurosci Methods 134:9–21.

Fan L, Li H, Zhuo J, Zhang Y, Wang J, Chen L, Jiang T (2016) The Human Brainnetome Atlas: a new brain atlas based on connectional architecture. Cereb Cortex 26:3508–3526.

Fransson P (2005) Spontaneous low-frequency BOLD signal fluctuations: an fMRI investigation of the resting-state default mode of brain function hypothesis. Hum Brain Mapp 26:15–29.

Glover GH, Li T-Q, Ress D (2000) Image-based method for retrospective correction of physiological motion effects in fMRI: RETROICOR. Magn Reson Med 44:162–167.

Greicius MD, Srivastava G, Reiss AL, Menon V (2004) Default-mode network activity distinguishes Alzheimer's disease from healthy aging: evidence from functional MRI. Proc Natl Acad Sci U S A 101:4637–4642.

Halassa MM, Sherman SM (2019) Thalamocortical circuit motifs: a general framework. Neuron 103:762–770.

Herrmann CS, Rach S, Neuling T, Strüber D (2013) Transcranial alternating current stimulation: a review of the underlying mechanisms and modulation of cognitive processes. Front Hum Neurosci 7:279.

Hillebrand A, Tewarie P, van Dellen E, Yu M, Carbo EW, Douw L, Stam CJ (2016) Direction of information flow in large-scale resting-state networks is frequency-dependent. Proc Natl Acad Sci U S A 113:3867–3872.

Hurley LM, Devilbiss DM, Waterhouse BD (2004) A matter of focus: monoaminergic modulation of stimulus coding in mammalian sensory networks. Curr Opin Neurobiol 14:488–495.

Hutchison RM, Womelsdorf T, Allen EA, Bandettini PA, Calhoun VD, Corbetta M, Chang C (2013) Dynamic functional connectivity: promise, issues, and interpretations. Neuroimage 80:360–378.

Jann K, Dierks T, Boesch C, Kottlow M, Strik W, Koenig T (2009) BOLD correlates of EEG alpha phase-locking and the fMRI default mode network. Neuroimage 45:903–916.

Kasten FH, Herrmann CS (2022) The hidden brain-state dynamics of tACS aftereffects. Neuroimage 264:119713.

Klimesch W, Sauseng P, Hanslmayr S (2007) EEG alpha oscillations: the inhibition-timing hypothesis. Brain Res Rev 53:63–88.

Knyazev GG, Slobodskoj-Plusnin JY, Bocharov AV, Pylkova LV (2011) The default mode network and EEG alpha oscillations: an independent component analysis. Brain Res 1402:67–79.

Korponay C, Janes AC, Frederick BB (2024) Brain-wide functional connectivity artifactually inflates throughout functional magnetic resonance imaging scans. Nat Hum Behav 8:1568–1580.

Kucyi A, Esterman M, Riley CS, Valera EM (2016) Spontaneous default network activity reflects behavioral variability independent of mind-wandering. Proc Natl Acad Sci U S A 113:13899–13904.

Leech R, Kamourieh S, Beckmann CF, Sharp DJ (2011) Fractionating the default mode network: distinct contributions of the ventral and dorsal posterior cingulate cortex to cognitive control. J Neurosci 31:3217–3224.

Leonardi N, Van De Ville D (2015) On spurious and real fluctuations of dynamic functional connectivity during rest. Neuroimage 104:430–436.

Li M, Gao Y, Anderson AW, Ding Z, Gore JC (2022) Dynamic variations of resting-state BOLD signal spectra in white matter. Neuroimage 250:118972.
Liu Z, He B (2008) fMRI–EEG integrated cortical source imaging by use of time-variant spatial constraints. Neuroimage 39:1198–1214.
Lopes da Silva F, Niedermeyer E (2005) Electroencephalography, basic principles, clinical applications and related fields.
Lurie DJ, Kessler D, Bassett DS, Betzel RF, Breakspear M, Kheilholz S, Calhoun VD (2020) Questions and controversies in the study of time-varying functional connectivity in resting fMRI. Netw Neurosci 4:30–69.
McCormick DA, Bal T (1997) Sleep and arousal: thalamocortical mechanisms. Annu Rev Neurosci 20:185–215.
Mitra PP, Pesaran B (1999) Analysis of dynamic brain imaging data. Biophys J 76:691–708.
Mo J, Liu Y, Huang H, Ding M (2013) Coupling between visual alpha oscillations and default mode activity. Neuroimage 68:112–118.
Osipova D, Ahveninen J, Jensen O, Ylikoski A, Pekkonen E (2005) Altered generation of spontaneous oscillations in Alzheimer's disease. Neuroimage 27:835–841.
Palva S, Palva JM (2007) New vistas for alpha-frequency band oscillations. Trends Neurosci 30:150–158.
Park J, Lindberg CR, Vernon FL (1987) Multitaper spectral analysis of high-frequency seismograms. Journal of Geophysical Research: Solid Earth 92:12675–12684.
Pedersen M, Zalesky A, Omidvarnia A, Jackson GD (2018) Multilayer network switching rate predicts brain performance. Proc Natl Acad Sci U S A 115:13376–13381.
Power JD, Barnes KA, Snyder AZ, Schlaggar BL, Petersen SE (2012) Spurious but systematic correlations in functional connectivity MRI networks arise from subject motion. Neuroimage 59:2142–2154.
Preti MG, Bolton TA, Van De Ville D (2017) The dynamic functional connectome: state-of-the-art and perspectives. Neuroimage 160:41–54.
Raichle ME, MacLeod AM, Snyder AZ, Powers WJ, Gusnard DA, Shulman GL (2001) A default mode of brain function. Proc Natl Acad Sci U S A 98:676–682.
Raichle ME, Snyder AZ (2007) A default mode of brain function: a brief history of an evolving idea. Neuroimage 37:1083–1090; discussion 1097-1089.
Richiardi J, Eryilmaz H, Schwartz S, Vuilleumier P, Van De Ville D (2011) Decoding brain states from fMRI connectivity graphs. Neuroimage 56:616–626.
Sadaghiani S, Kleinschmidt A (2016) Brain networks and α-oscillations: structural and functional foundations of cognitive control. Trends Cogn Sci 20:805–817.
Samogin J, Liu Q, Marino M, Wenderoth N, Mantini D (2019) Shared and connection-specific intrinsic interactions in the default mode network. Neuroimage 200:474–481.
Scheeringa R, Petersson KM, Kleinschmidt A, Jensen O, Bastiaansen MCM (2012) EEG alpha power modulation of fMRI resting-state connectivity. Brain Connect 2:254–264.
Shakil S, Lee C-H, Keilholz SD (2016) Evaluation of sliding window correlation performance for characterizing dynamic functional connectivity and brain states. Neuroimage 133:111–128.
Shanahan M (2010) Metastable chimera states in community-structured oscillator networks. Chaos 20:013108.
Shirer WR, Ryali S, Rykhlevskaia E, Menon V, Greicius MD (2012) Decoding subject-driven cognitive states with whole-brain connectivity patterns. Cereb Cortex 22:158–165.
Tagliazucchi E, von Wegner F, Morzelewski A, Brodbeck V, Laufs H (2012) Dynamic BOLD functional connectivity in humans and its electrophysiological correlates. Front Hum Neurosci 6:339.
Tang W, Liu H, Douw L, Kramer MA, Eden UT, Hamalainen MS, Stufflebeam SM (2017) Dynamic connectivity modulates local activity in the core regions of the default-mode network. Proc Natl Acad Sci U S A 114:9713–9718.
Tu PC, Bai YM, Li C-T, Chen M-H, Lin W-C, Chang WC, Su T-P (2019) Identification of common thalamocortical dysconnectivity in four major psychiatric disorders. Schizophr Bull 45:1143–1151.
Varela F, Lachaux J-P, Rodriguez E, Martinerie J (2001) The brainweb: phase synchronization and large-scale integration. Nat Rev Neurosci 2:229–239.
Vergara VM, Abrol A, Calhoun VD (2019) An average sliding window correlation method for dynamic functional connectivity. Hum Brain Mapp 40:2089–2103.
Vollenweider FX, Preller KH (2020) Psychedelic drugs: neurobiology and potential for treatment of psychiatric disorders. Nat Rev Neurosci 21:611–624.
Whitfield-Gabrieli S, Thermenos HW, Milanovic S, Tsuang MT, Faraone SV, McCarley RW, LaViolette P (2009) Hyperactivity and hyperconnectivity of the default network in schizophrenia and in first-degree relatives of persons with schizophrenia. Proc Natl Acad Sci U S A 106:1279–1284.
Yuan H, Zotev V, Phillips R, Bodurka J (2013) Correlated slow fluctuations in respiration, EEG, and BOLD fMRI. Neuroimage 79:81–93.